Pharm Res (2013) 30:3059–3076
DOI 10.1007/s11095-013-1038-z

RESEARCH PAPER

Toward the Establishment of Standardized *In Vitro* Tests for Lipid-Based Formulations, Part 3: Understanding Supersaturation *Versus* Precipitation Potential During the *In Vitro* Digestion of Type I, II, IIIA, IIIB and IV Lipid-Based Formulations

Hywel D. Williams • Philip Sassene • Karen Kleberg • Marilyn Calderone • Annabel Igonin • Eduardo Jule • Jan Vertommen • Ross Blundell • Hassan Benameur • Anette Müllertz • Colin W. Pouton • Christopher J. H. Porter • on behalf of the LFCS Consortium

Received: 9 January 2013 / Accepted: 25 March 2013 / Published online: 10 May 2013

ABSTRACT

Purpose Recent studies have shown that digestion of lipid-based formulations (LBFs) can stimulate both supersaturation and precipitation. The current study has evaluated the drug, formulation and dose-dependence of the supersaturation – precipitation balance for a range of LBFs.

Methods Type I, II, IIIA/B LBFs containing medium-chain (MC) or long-chain (LC) lipids, and lipid-free Type IV LBF incorporating different doses of fenofibrate or tolfenamic acid were digested *in vitro* in a simulated intestinal medium. The degree of supersaturation was assessed through comparison of drug concentrations in aqueous digestion phases (AP_{DIGEST}) during LBF digestion and the equilibrium drug solubility in the same phases.

Results Increasing fenofibrate or tolfenamic acid drug loads (*i.e.*, dose) had negligible effects on LC LBF performance during digestion, but promoted drug crystallization (confirmed by XRPD) from MC and Type IV LBF. Drug crystallization was only evident in instances when the calculated maximum supersaturation ratio (SR^M) was >3. This threshold SR^M value was remarkably consistent across all LBF and was also consistent with previous studies with danazol.

Conclusions The maximum supersaturation ratio (SR^M) provides an indication of the supersaturation 'pressure' exerted by formulation digestion and is strongly predictive of the likelihood of drug precipitation *in vitro*. This may also prove effective in discriminating the *in vivo* performance of LBFs.

KEY WORDS bioavailability · drug solubilization · *in vitro* digestion testing · *in vitro* models · LFCS Consortium · lipid-based drug delivery systems · precipitation · SEDDS · solubility · supersaturation

INTRODUCTION

Lipid-based formulations (LBFs) are a viable strategy to enhance drug absorption in the gastro-intestinal (GI) tract in

Electronic supplementary material The online version of this article (doi:10.1007/s11095-013-1038-z) contains supplementary material, which is available to authorized users.

H. D. Williams · C. J. H. Porter (✉)
Drug Delivery, Disposition and Dynamics
Monash Institute of Pharmaceutical Sciences
Parkville, Victoria 3052, Australia
e-mail: chris.porter@monash.edu

P. Sassene · K. Kleberg · A. Müllertz
Department of Pharmaceutics, Faculty of Health and Medical Sciences
University of Copenhagen, Universitetsparken 2
DK-2100 Copenhagen, Denmark

M. Calderone · R. Blundell
Sanofi Research and Development, Montpellier, France

A. Igonin · J. Vertommen · H. Benameur
Capsugel R&D, Strasbourg, France

E. Jule
Capsugel Product Development Center
Cambridge, Massachusetts, USA

C. W. Pouton (✉)
Drug Discovery Biology, Monash Institute of Pharmaceutical Sciences
Parkville, Victoria 3052, Australia
e-mail: colin.pouton@monash.edu

Present Address:
H. D. Williams
Capsugel R&D, Strasbourg, France

instances where low aqueous drug solubility and/or poor dissolution limit exposure (1–3). LBFs can increase drug absorption through several well-described processes. These include presentation of drug to the GI tract in a pre-dissolved form (4, 5), enhancement of drug solubilization in the intestinal milieu (6), and increased intestinal drug permeability (7–9). For some highly lipophilic drugs, LBFs may also increase bioavailability *via* promotion of intestinal lymphatic transport (10, 11) and a decrease in first pass metabolism in the enterocyte or liver (12, 13). In addition, there is growing interest in the role played by supersaturation in drug absorption from LBFs, as well as other enabling formulations such as amorphous solid dispersions (14–16). Supersaturation has the potential to increase drug absorption, as the attainment of drug concentrations in the GI tract that are in excess of crystalline drug solubility is expected to enhance absorptive flux. Conversely, supersaturated drug is thermodynamically unstable and may also precipitate to the more slowly dissolving crystalline solid prior to absorption. Ideal supersaturating formulations therefore maintain drug in the supersaturated state for a period of time sufficient for absorption to occur (16).

LBFs generate supersaturation *in vivo* because the solubilization capacity of the formulation usually drops during dispersion in the gastric and intestinal fluids, and digestion in the small intestine (17). Formulation dispersion lowers the solubilization capacity of LBFs that contain larger quantities of hydrophilic surfactants and cosolvents as these components readily partition into the bulk aqueous phase. Enzymatic hydrolysis of digestible lipids and fatty acid ester surfactants by gastric and intestinal secretions subsequently reduces solubilization capacity further, promoting ongoing supersaturation. Finally, recent evidence indicates that dilution with bile salt micelles (and conversion of lipid-rich colloids to bile salt-rich colloids), together with a reduction in colloidal lipid content stimulated by lipid absorption in the acidic unstirred water-layer, may also promote supersaturation (18,19)

The decrease in LBF solubilization capacity during *in vivo* processing creates the necessary imbalance between the initial solubilized drug concentration in the GI fluids (which in the absence of precipitation is related to the dose) and drug solubility in the colloidal species formed post dispersion/digestion. The degree of supersaturation attained is critically important (14,20) as increasing supersaturation and thermodynamic instability leads to a greater likelihood of crystallization from supersaturated solutions (21,22). Knowledge of the degree of supersaturation attained following dispersion and digestion of LBF, and identification of formulations that are destined to generate high degrees of supersaturation (and therefore a high risk of crystallization) is expected to facilitate more rational LBF development. Improved *a priori* predictions of *in vivo* LBF performance are increasingly possible through the conduct of *in vitro* dispersion and digestion tests (14, 23, 24), however widespread use of these tests has been hampered by the lack of standardized test conditions. This is the current focus of the LFCS Consortium, a not-for-profit organization of groups in academia and industry with common interests in standardized *in vitro* testing methods for LBFs (25).

Previous studies from the Consortium (20,25,26) provide preliminary guidance on LBF testing, including suggestions for the appropriate bile salt type and concentration, the pancreatic extract enzymatic activity and the importance of assessing the degree of supersaturation in evaluating LBF performance. However, these studies were limited to the evaluation of danazol-containing LBFs. The present study has explored, under a range of experimental conditions, the performance of LBFs containing two alternative model compounds - fenofibrate (a highly lipophilic neutral compound) and tolfenamic acid (a poorly water-soluble weak acid). The data obtained highlight the importance of LBF drug loading relative to the drug solubility in the digested LBF as a driver of formulation performance. This relationship dictates the degree of supersaturation generated on digestion, and therefore, the likelihood that supersaturation will lead to rapid drug precipitation rather than enhanced drug absorption.

MATERIALS AND METHODS

Materials

Maisine™ 35–1 and Transcutol® HP were supplied by Gattefossé (Saint-Priest, France). Captex® 300 and Capmul® MCM EP were supplied by Abitec Corp (Columbus, OH). Cremophor® EL was a gift from BASF Corporation (Washington, NJ). Corn oil, Tween® 85, fenofibrate, tolfenamic acid, sodium taurodeoxycholate >95% (NaTDC), 4-bromophenylboronic acid and the porcine pancreatin extract (P7545, 8×USP specifications activity) were all obtained from Sigma Chemical Co. (St Louis, MO). Further details of the lipidic excipients used within LFCS Consortium can be found in our earlier work (25). Phosphatidylcholine (PC) (Lipoid E PC S, approximately 99.2% pure, from egg yolk) was obtained from Lipoid (Lipoid GmbH, Ludwigshafen, Germany). 1 M sodium hydroxide, was diluted to obtain 0.2 M and 0.6 M NaOH titration solutions, and was purchased from Merck (Darmstadt, Germany). Water was obtained from a Milli-Q water purification system (Millipore, Bedford, MA).

Selection of LBFs for Investigation in the LFCS Consortium

The compositions of the eight concept lipid-based formulations (LBFs) investigated by the LFCS Consortium are shown in Fig. 1. The equilibrium solubility of fenofibrate

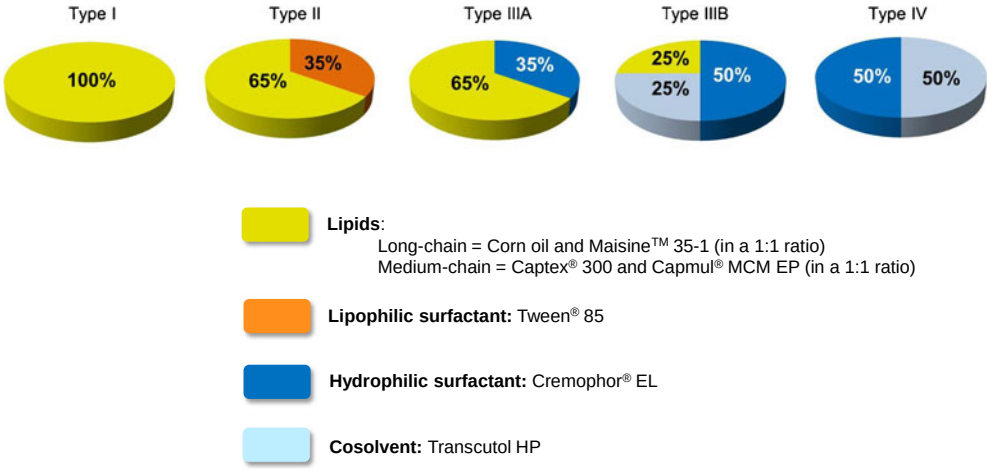

Fig. 1 The composition of the 8 lipid-based formulations (LBFs) investigated by the LFCS Consortium**.** LC; long-chain. MC; medium-chain. In the LC LBFs, the lipids consisted of corn oil:Maisine™ 35–1 in a 1:1 w/w ratio. In the Type I, II and IIIA MC LBFs, the lipid consisted of Captex 300:Capmul MCM EP, in a 1:1 w/w ratio. Capmul® was the only lipid in the Type IIIB MC LBF. Corn oil and Captex® 300 are triglycerides of LC and MC lipids, respectively. Maisine™ 35–1 and Capmul® MCM EP are blends of predominantly mono- and diglyceride and some triglyceride, of LC and MC lipids respectively. Tween® 85 is a polyoxyethylene sorbitan trioleate surfactant (HLB 11). Cremophor® EL is a polyethoxylated castor oil surfactant (HLB 14–16). Transcutol HP is diethylene glycol monoethyl ether cosolvent. LBFs were classified according to the Lipid Formulation Classification System (17).

and tolfenamic acid in each LBF was determined at 37°C using a method described previously (25).

Drug Incorporation into the LBFs

LBFs were loaded with fenofibrate or tolfenamic acid at between 20% and 100% of the saturated solubility of the drug in the LBF. The required mass of drug was weighed directly into clean screw-top glass vials and drug-free LBF was added up to the target mass loading. Vials were sealed, vortex-mixed and incubated at 37°C for at least 24 h prior to testing. The drug content in each manufactured LBF was verified (in triplicate) on the day of testing when accurately weighed samples were removed from the vial, transferred to 5 ml volumetric flasks and made up to volume with chloroform:methanol (2:1, v/v). Aliquots (50 μl) were diluted >10 fold with acetonitrile and analyzed for drug content by HPLC (see "HPLC Detection of Model Drugs" section below for details).

In Vitro Evaluation of the LBFs

Digestion Experiments

In vitro digestion experiments were performed as described previously by Williams *et al.* (25). In brief, the experimental set-up employed by the LFCS Consortium consisted of a pH-stat apparatus (Metrohm® AG, Herisau, Switzerland), comprising a Titrando 802 propeller stirrer/804 Ti Stand combination, a glass pH electrode (iUnitrode) and two 800 Dosino dosing units coupled to 10 ml autoburettes (Metrohm® AG, Herisau, Switzerland). The apparatus was connected to a PC and operated using Tiamo 2.0 software (Metrohm® AG). The digestion buffer (pH 6.5) contained 2 mM Tris-maleate, 1.4 mM $CaCl_2 \cdot 2H_20$ and 150 mM NaCl, and was supplemented with 3 mM NaTDC and 0.75 mM PC.

LBF (1.083 ± 0.025 g) was weighed directly into a thermostat-jacketed glass reaction vessel (Metrohm® AG, Herisau, Switzerland) and dispersed for 10 min in 39 ml digestion medium (37°C). Continuous mixing during was achieved using an overhead propeller stirrer 25 mm in diameter and rotating at a speed of ~450 min^{-1}. The pH of the media during the initial dispersion phase was manually adjusted to pH 6.5 ± 0.05 using small quantities of NaOH or HCl. During this dispersion phase, 3 × 1 ml samples were removed for analysis of solubilized drug content (see "Collection and Separation of Samples Removed During *In Vitro* Digestion Testing") to leave 1 g LBF and 36 ml of digestion medium. Digestion was subsequently initiated *via* addition of 4 ml pancreatin from porcine pancreas extract prepared as described previously (25). Sodium hydroxide titration solutions (titrants) of 0.2 M and 0.6 M were utilized for digests containing LC and MC LBF, respectively, and were automatically added (controlled *via* the pH stat controller) to the reaction vessel to maintain constant pH during digestion, with the rate of titrant addition reflecting the digestibility of the LBF. Digestion tests were terminated after 30 min or 60 min, depending on the composition of the LBF.

Collection and Separation of Samples Removed During In Vitro Digestion Testing

Digestion samples were immediately treated with a digestion inhibitor (5 μL of 1.0 M 4-bromophenylboronic acid in

methanol per 1 ml of digestion medium) to arrest digestion. Samples were then separated by centrifugation into three phases, namely a poorly dispersed oily phase (if present, consisting primarily of undigested lipids), a dispersed aqueous colloidal phase (AP_{DIGEST}; consisting of swollen bile salt/phospholipid mixed micelles and vesicles) and a precipitated pellet phase. In line with previous recommendations (25), ultracentrifugation (400,000*g*, Optima XL-100 K centrifuge, SW-60 rotor, Beckman, Palo Alto, CA) was used for LBFs generating an oil-phase post-separation of the digestion samples and a bench-top centrifuge (21,000*g*, Fresco 21, Heraeus®, Thermo Scientific, Langenselbold, Germany) used for all other LBFs. The suitability of the bench-top centrifuge for separating fenofibrate and tolfenamic acid precipitate was confirmed in preliminary experiments (see Fig S1 of the Supplementary Material). The digestion phases were isolated as described previously (25) and analyzed for drug content by HPLC (see section "HPLC Detection of Model Drugs").

Samples removed after 5 and 10 min of initial dispersion (non-digestion conditions) were immediately centrifuged (21,000*g*) at 37°C for 10 min using a bench-top centrifuge (Fresco 21, Heraeus®). Samples post-centrifugation consisted of an aqueous phase (AP_{DISP}), and a phase-separated oil phase in instances where the LBF showed poor dispersion properties or a pellet phase in instances where drug precipitation commenced during dispersion. Aliquots (50–100 μl) of the AP_{DISP} were removed and diluted >10-fold with acetonitrile before analysis for drug content by HPLC (see section "HPLC Detection of Model Drugs"). An additional, non-centrifuged 1 ml sample collected between the 5 and 10 min dispersion time points was dissolved with acetonitrile and a small volume (<1 ml) of chloroform:methanol (2:1, v/v) in instances where the acetonitrile could not dissolve all of the lipid content of the sample. After mixing, an aliquot of this sample was diluted >10-fold in acetonitrile and assayed for drug by HPLC (see section "HPLC Detection of Model Drugs"). The measured concentration in this sample was used to verify the maximum drug concentrations in the *in vitro* digestion test (AP_{MAX}).

Determination of Drug Solubility in Colloidal Aqueous Phases Post-Dispersion (AP_{DISP}) and Post-Digestion (AP_{DIGEST})

The solubility of fenofibrate and tolfenamic acid in the colloidal aqueous phase (AP) generated by dispersion and digestion of blank (*i.e.* drug free) LBF was evaluated under the conditions described in the "Digestion Experiments" section above. Samples were removed after 10 min dispersion and after various times of digestion over 60 min. Samples were treated in the same manner as the those described in the "Collection and Separation of Samples Removed During *In Vitro* Digestion" section above (where bench-top centrifugation was used for the dispersion samples and digestion samples not containing an oil phase, and ultracentrifugation used in all other instances).

Samples (~1 ml) of the AP_{DISP}/AP_{DIGEST} were transferred to Eppendorf® tubes that contained excess crystalline drug. Vials were briefly vortex-mixed and incubated at 37°C. At time intervals, mixtures were centrifuged (21,000 *g*, Heraeus® Fresco 21) at 37°C for 10 min to sediment undissolved drug and 50–100 μL of the clear supernatant was removed and diluted with acetonitrile prior to analysis (see section "HPLC Detection of Model Drugs"). Solubility in the AP_{DISP} and AP_{DIGEST} was repeatedly assessed over a 4 h period of equilibration. During the equilibration period, the pH of samples containing tolfenamic acid was frequently assessed and adjusted to pH 6.5 ±0.01 using small volumes of NaOH. Solubility values were used to calculate the supersaturation ratio (SR) obtained during digestion *via* Eq. 1:

$$SR = \frac{\text{solubilized drug concentration in } AP_{DIGEST}}{\text{drug solubility in } AP_{DIGEST}} \quad (1)$$

Equation 2 was used to calculate the maximum supersaturation ratio (SR^M), which is the ratio between the maximum theoretical concentration of solubilized drug (in the absence of any drug precipitation; AP_{MAX}) and drug solubility in the AP_{DIGEST}:

$$SR^M = \frac{\text{maximum drug concentration in } (AP_{MAX})}{\text{drug solubility in } AP_{DIGEST}} \quad (2)$$

SR^M provides an indication of the maximum supersaturation pressure within each test (20) since it compares the maximum drug concentration that may be attained in the test to the lowest solubility value *i.e.*, at the end of the digestion tests (60 min in most cases).

HPLC Detection of Model Drugs

All HPLC analyses were conducted using a Waters Alliance 2695 Separation Module (Waters Alliance Instruments, Milford, MA) with a reverse-phase C_{18} column (150×3.9 mm, 5 μm, Waters Symmetry®) and C_{18} security guard cartridge (4×2.0 mm, Phenomenex, Torrence, CA). The UV detection for fenofibrate and tolfenamic acid was at 286 nm and 290 nm respectively. For both compounds, the injection volume was 50 μl, the mobile phase consisted of acetonitrile and water in a 80:20 v/v ratio with 0.1% (v/v) formic acid and was pumped through the column at a 1 ml/min flow rate.

Assays were validated following analysis of 5 quality control samples made up at three different concentrations

(0.5 μg/ml, 5 μg/ml and 25 μg/ml). Intra-assay validation for fenofibrate revealed accuracies of 97.0%, 99.4% and 99.8% and precision to within 0.5%, 1.0% and 0.4% of the target. Inter-assay validation (over 3 days) for fenofibrate revealed accuracies of 97.8%, 101.2% and 100.0% and precision to within 1.3%, 1.8% and 1.7% of the target. Intra-assay validation for tolfenamic acid revealed accuracies of 91.0%, 99.9% and 99.7% and precision to within 2.4%, 3.0% and 2.3% of the target. Inter-assay validation (over 3 days) for tolfenamic acid revealed accuracies of 94.7%, 100.3% and 100.2% and precision to within 6.0%, 2.6% and 2.0% of the target. Fenofibrate mean recoveries from spiked digestion phases were 103.4±1.8% from the oil phase (n=6), 99.9±2.4% from the AP_{DIGEST} (n=12) and 98.4 ±1.0% from the pellet phase (n=6). Tolfenamic acid mean recoveries from spiked digestion phases were 99.8±7.7% from the oil phase (n=12), 100.7±8.0% from the AP_{DIGEST} (n=12) and 92.8±2.2% from the pellet phase (n=12).

Solid-State Analysis of the Pellet Phase

Polarized Light Microscopy

Selected digestion pellets containing precipitated fenofibrate or tolfenamic acid were analyzed using a Zeiss Axiolab microscope (Carl Zeiss, Oberkochen, Germany) equipped with crossed polarizing filters. The pellet was carefully removed from the sample tube and placed on a microscope slide. Samples were analyzed under cross-polarized light, and images were recorded using a Canon PowerShot A70 digital camera (Canon, Tokyo, Japan). Pellets were isolated and analyzed in the manner described above on the same day (typically within 2 h of sampling) to minimize the risk of changes in drug crystal habit during storage

X-ray Powder Diffraction (XRPD)

Selected digestion pellets were also examined by XRPD in order to determine the solid-state form of precipitated fenofibrate/tolfenamic acid and to verify the observations made using the polarized light microscope. Digestion pellets were mounted onto a poly(methyl methacrylate) back loading sample holder ready for analysis. The instrument was a Bruker D8 Advance powder diffractometer (Bruker, Sydney, Australia) with a copper tube anode and Kα radiation source (= 1.542 Å). The applied voltage and current were 45 kV and 40 mA respectively. The samples were scanned between 5° and 40° (2θ), with a step size of 0.02° and a scanning speed of 2 s/step. The diffractograms were prepared using the DIFFRAC^{PLUS} software (Bruker). The time period between sampling of the digestion pellet and XRPD analysis was less than 24 h.

RESULTS

Fenofibrate and Tolfenamic Acid Equilibrium Solubility in the LBFs

The equilibrium solubilities of fenofibrate and tolfenamic acid in the eight investigated LBFs are shown in Fig. 2. Chemical structure, log P, melting temperature and aqueous solubility is also reported. Fenofibrate solubility ranged from 98.1 mg/g in the Type I-LC LBF to 189.1 mg/g in the Type IV LBF. Fenofibrate solubility across the eight LBFs therefore varied by almost 100%. However, solubility across the Type I-IIIA LBF, which were the more lipid-rich and cosolvent free LBFs, varied by only ~8% and ~10% for LC and MC LBFs, respectively. Fenofibrate solubility was slightly higher in the MC formulations and very high in the Type IV LBF, reflecting the very high solubility of fenofibrate in Transcutol (243.8±21.4 mg/g).

Consistent with fenofibrate, tolfenamic acid solubility was lowest in the Type I-LC LBF (8.8 mg/g), highest in formulations containing Transcutol (*i.e.*, Type IIIB-MC and IV LBF), and higher in the MC when compared to LC lipid formulations. Tolfenamic acid solubilities were in general 3–10 fold lower than the equivalent fenofibrate values.

Effect of Fenofibrate and Tolfenamic Acid on *In Vitro* Digestion of the LBFs

Figure 3 compares the volumes of NaOH added during *in vitro* digestion of Type II and IIIA LBF containing fenofibrate/tolfenamic acid (at 80% saturation), to the volume added during digestion of drug-free LBF (see Fig. S2 and S3 of the Supplementary Material for equivalent plots for the remaining four LBFs). The volumes of NaOH added during the testing of fenofibrate-containing LBF and drug-free LBF were comparable. The slightly lower volumes added in the presence of fenofibrate can be attributed to the displacement of a proportion of the mass of lipid in the LBF (on a weight for weight basis) by fenofibrate which decreases the amount of lipid substrate in the experiments (20). This becomes noticeable for fenofibrate-containing formulations by virtue of its very high lipid solubility.

Tolfenamic acid also had a negligible effect digestion during the testing of Type II-MC and IIIA-MC LBF, although higher volumes of NaOH were added during the testing of drug containing LC LBF. At first glance this suggests that tolfenamic acid was enhancing LBF digestion. However, an alternative explanation, namely that the drug was directly affecting pH in the tests (and, therefore, titration), was also explored since the pK_a of tolfenamic acid of ~4.1 (32) suggests that over 99% was ionized at pH 6.5. The capacity for ionized tolfenamic acid to lower pH in the

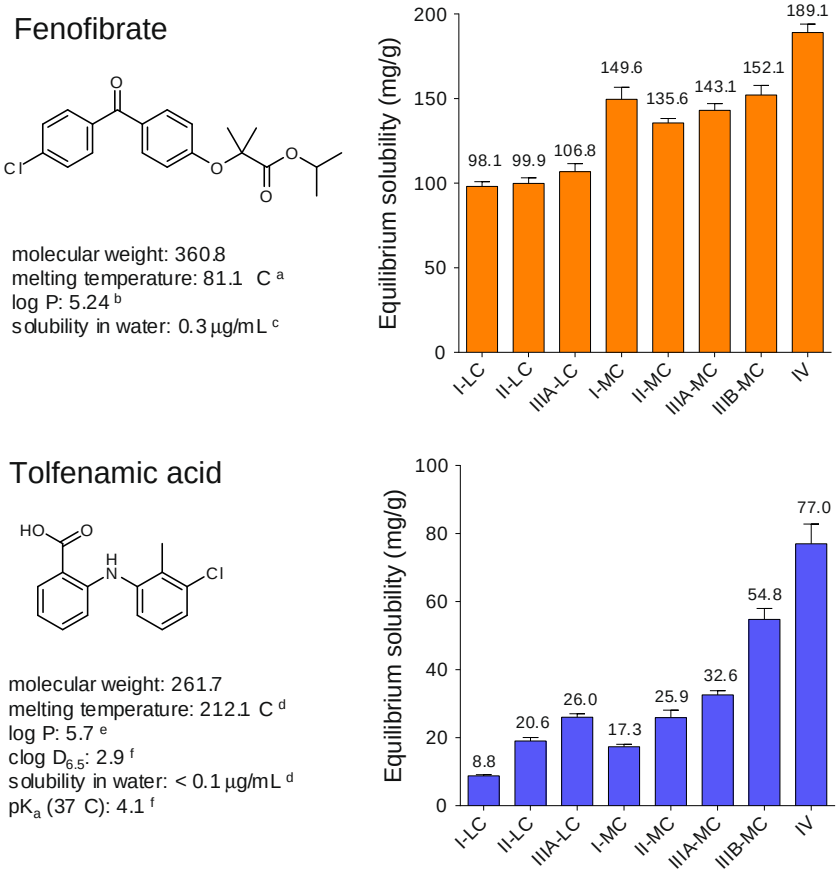

Fig. 2 Equilibrium solubility values for fenofibrate and tolfenamic acid in the eight investigated lipid-based formulations (LBFs) arranged in order of LBF type. Solubility determinations were performed at 37°C over 72 h. Values are expressed as means ($n = 3$) ± 1 SD. The formulation compositions can be found in Fig. 1. MC, medium chain; LC, long chain. The chemical structure of the drugs and selected physicochemical properties are also shown. [a] Van Speybroeck *et al.* (27). [b] Munoz *et al.* (28). [c] Vogt *et al.* (29) [d] Bergstrom *et al.* (30). [e] Osterberg *et al.* (31). [f] Fagerberg *et al.* (32).

digestion test was confirmed in experiments that revealed a correlation between tolfenamic acid load in the LBF and pH changes in the digestion medium (Fig. S4 of the Supplementary Material). Therefore, the higher NaOH volumes added during *in vitro* digestion of tolfenamic acid-containing LBFs may also reflect the dissociation of tolfenamic acid as the digestion of the oil droplet phase forced more drug to enter the aqueous phase. Similar effects were less evident during digestion of MC LBFs, but may reflect the greater absolute change in pH due to increased digestion of the MC lipids, masking the more subtle effects of tolfenamic acid on media pH.

Effect of *In Vitro* Digestion on the Drug Solubilization Properties of LC and More Slowly Digesting Type I-MC LBFs

The effect of *in vitro* digestion of Type I-LC, II-LC, IIIA-LC and I-MC LBFs on the fate of incorporated fenofibrate and tolfenamic acid is shown in Fig. 4a and b, respectively. LBFs were loaded with drug at 80% and 100% of the saturated solubility values in Fig. 2. Upper panels in Fig. 4a and b show the % drug distribution across the poorly dispersed oil phase, the AP_{DIGEST} and the pellet isolated after 30 min digestion. The lower panels show the drug concentrations measured in the AP_{DIGEST} at 30 min during a kinetic digestion experiment, and compare this to the drug solubility in the same AP_{DIGEST} colloids (*i.e.*, the solubilization capacity). The latter is represented by the dashed horizontal line. Supersaturation ratios at 30 min digestion were calculated using Eq. 1 and are shown in red.

Type I-MC, I-LC and II-LC LBFs contain only water-immiscible components, and as such form coarse dispersions (in the case of Type I) or turbid emulsions (in the case of Type II) in the digestion medium. The low water solubility of the lipid components in these formulations (and their digestion products) also limits the extent of digestion *in vitro* (20,25) since the solubilization capacity of the test medium for the digestion products is typically exceeded before complete digestion occurs, effectively poisoning on-going digestion. This dictates that the most lipophilic LBFs retain more of the solubilization properties of their initial dispersed forms when compared to the more hydrophilic formulations. The incomplete digestion of Type I-MC, I-LC and II-LC LBFs, results in facile phase-separation of the undigested and poorly dispersed oil phase during centrifugation. As evident in Fig. 4a (upper panels), the majority of the incorporated fenofibrate was recovered from this lipid phase. The high affinity of fenofibrate for the lipid components of the Type I-MC, I-LC and II-LC LBFs limited drug concentrations in the AP_{DIGEST}, resulting in lower supersaturation ratios (lower panels; Fig. 4a).

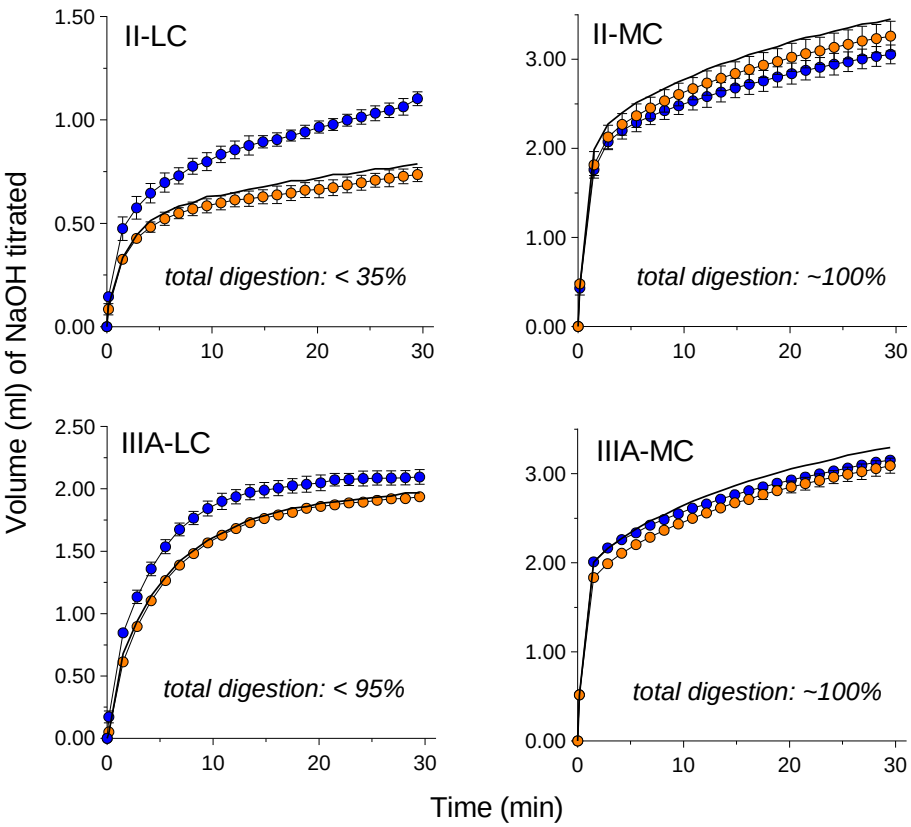

Fig. 3 Effect of incorporated tolfenamic acid (●) or fenofibrate (●) on the volume of NaOH added during *in vitro* digestion of Type II and IIIA lipid-based formulations (LBFs) containing long-chain (LC) or medium-chain (MC) lipids. The NaOH concentration was 0.2 M for LC formulations and 0.6 M for MC formulations. Values are expressed as means ($n=3$) ± 1 SD. The LBF compositions can be found in Fig. 1. Drug was incorporated at 80% of the drug solubility in the formulation (shown in Fig. 2). The solid line represents the digestion of the blank (drug-free) LBF. The effect of incorporated fenofibrate/tolfenamic acid on the digestion of all other LBFs are shown in Fig. S2 and S3 of the Supplementary Material. Estimates for total LBF digestion are taken from Williams *et al.* (25).

In contrast, following digestion of equivalent tolfenamic acid containing LBFs (Fig. 4b), higher proportions of drug were present in the AP_{DIGEST}. This presumably reflected ionization of tolfenamic acid at the pH of the digestion medium (the pK_a of tolfenamic is 4.1 (32)), effectively lowering drug affinity for the lipid phase. The high aqueous solubility of ionized tolfenamic acid also contributed to the lower supersaturation ratios (lower panels; Fig. 4b) and reduced risks of precipitation.

The Type IIIA-LC LBF is more hydrophilic and readily disperses to form an ultrafine oil in water dispersion in aqueous media (25). The higher surfactant content also increases the solubilization capacity of the digestion medium and affords close to complete digestion under the standard LFCS Consortium digestion conditions (20,25). From the measured drug solubilities in the dispersed (*i.e.*, AP_{DISP}) and digested LBF (*i.e.*, AP_{DIGEST}), it is apparent that the digestion of the Type IIIA-LC LBF resulted in a significant drop in solubilization capacity, from 1.7±0.2 mg/ml on dispersion to 0.7±0.2 mg/ml after 30 min digestion. As fenofibrate concentrations in the digestion tests at fenofibrate loadings of 85 mg and 107 mg (representing 80% and 100% of the saturated fenofibrate solubility in the Type IIIA-LC LBF, respectively) were higher than the solubilization capacity of the AP_{DISP} and the AP_{DIGEST}, there was evidence of supersaturation during both dispersion and digestion, with the lower solubilization capacity of the AP_{DIGEST} giving rise to higher supersaturation ratios during the digestion phase (SR=2.8 and 3.0 at 80% and 100% loadings in the formulation, respectively). The paucity of drug precipitation, however, indicates that the supersaturated solution generated was relatively stable over the 30 min digestion period. Additional tests (data not shown) confirmed that, for this LBF, supersaturation could be maintained for at least 60 min.

The equivalent IIIA-LC LBF containing tolfenamic also showed negligible precipitation on digestion (Fig. 4b). The lower solubility of tolfenamic acid in the LBF (compared to fenofibrate), however, resulted in lower drug loadings, lower drug concentrations in the AP_{DIGEST} and an attenuated degree of supersaturation (SR=1.0 and 1.2 at 80% and 100%, respectively).

Effect of *In Vitro* Digestion on the Drug Solubilization Properties of Rapidly Digesting MC and Type IV LBFs

Fenofibrate Containing LBFs

Figure 5 shows the solubilized concentrations of fenofibrate during a 10 min dispersion phase and a 60 min period of digestion of Type II-MC, IIIA-MC, IIIB-MC and IV LBFs containing drug at 20%, 40%, 60% and 80% of saturated solubility in the formulation. A longer experimental duration and higher sample frequency was employed in these experiments as the digestion of Type II-MC, IIIA-MC, IIIB-MC and IV LBFs led to higher degrees of supersaturation

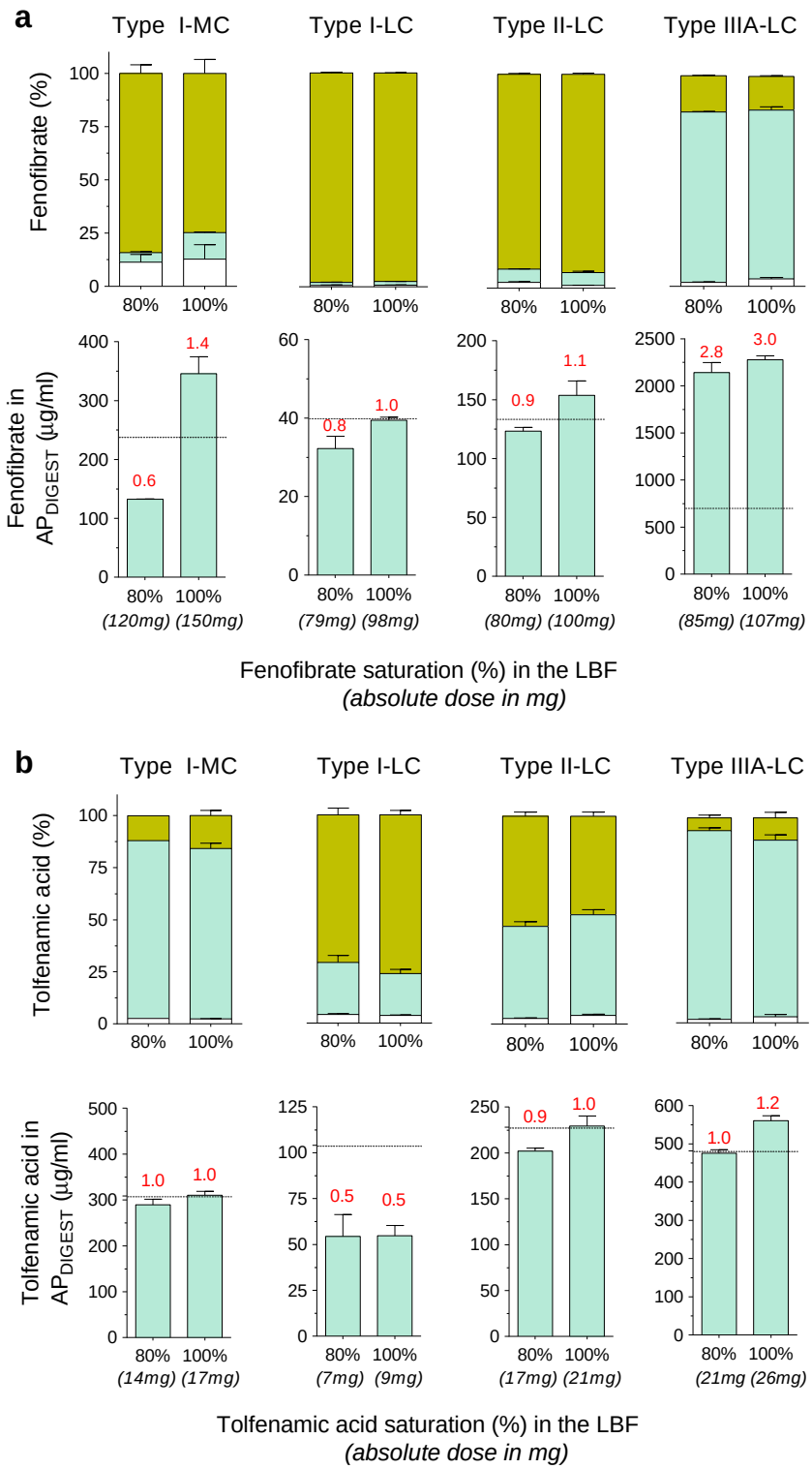

Fig. 4 The effect of *in vitro* digestion (30 min) on the performance of Type I-LC, II-LC, IIIA-LC and I-MC lipid-based formulations (LBFs) containing (**a**) fenofibrate and (**b**) tolfenamic acid. The composition of the formulations is shown in Fig. 1. LBFs contained fenofibrate at 80% and 100% of the drug solubility in the formulation. *Upper panels* plot the% distribution of drug across a poorly dispersed oil phase (*yellow bars*), a colloidal aqueous phase [(AP_{DIGEST}) blue bars] and a pellet phase (*white bars*). The lower panels plot the solubilized drug concentrations in the AP_{DIGEST}. All values are expressed as means ($n = 3$) ± 1 SD. The dashed horizontal line represents the solubilization capacity in the AP_{DIGEST} (*i.e.*, the solubility of crystalline drug in this phase) and values in red are the supersaturation ratios according to Eq. 1.

and sustained precipitation. The dashed black line in Fig. 5 traces the solubilization capacity of the dispersed (AP_{DISP}) and digested LBF (AP_{DIGEST}). Concentrations above this line are therefore supersaturated.

As the self-emulsification properties of the Type II-MC LBF were relatively poor, the formulation phase-separated on centrifugation to form an incompletely dispersed oily phase. Drug concentrations in the AP_{DISP} were accordingly lower than expected. Total solubilized drug concentrations (*i.e.*, drug present in the AP_{DISP} plus the phase-separated oil phase) are represented in Fig. 5a by the dashed colored lines. The solubilization capacity of the Type II-MC LBF

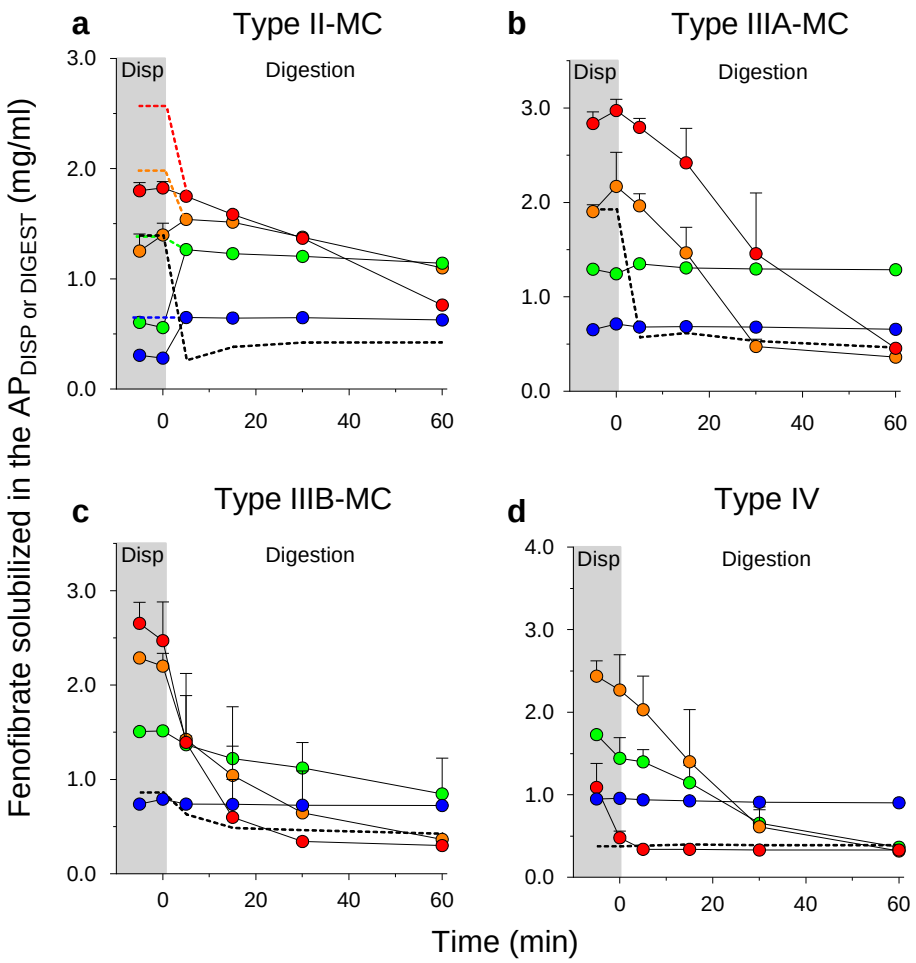

Fig. 5 The effect of fenofibrate saturation level in Type II-MC, IIIA-MC, IIIB-MC and IV lipid-based formulations (LBFs) on drug solubilization during 60 min *in vitro* digestion. Formulations contained fenofibrate at 80% (●), 60% (●), 40% (●) and 20% (●) of solubility in the formulation. Formulation compositions are shown in Fig. 1. All values are expressed as means ($n = 3$) ± 1 SD. The dashed black line represents the solubilization capacity of the aqueous phase during LBF dispersion (AP_{DISP}) and digestion (AP_{DIGEST}). The dashed colored lines in panel a represent the total solubilized concentration of fenofibrate (drug in AP_{DISP} plus the phase-separated oil phase)

during the dispersion phase was 1.40 ± 0.1 mg/ml, but decreased 5-fold to 0.27 ± 0.1 mg/ml after only 5 min of digestion (AP_{DIGEST_5MIN}). Critically, the decrease in LBF solubilization capacity was sufficient to create supersaturation at each fenofibrate loading (Fig. 5a). While there was evidence of decreasing solubilized fenofibrate concentrations at the higher drug loadings (*i.e.*, 60% and 80%), the absence of precipitation at lower loadings (*i.e.*, 20% and 40%) confirmed that lower degrees of supersaturation could be maintained during digestion.

Dispersion of the Type IIIA-MC LBF led to supersaturation only at the higher 60% and 80% drug loads (Fig. 5b). After 5 min of digestion, however, supersaturation was also attained at the lower 20% and 40% loadings. Consistent with the Type II-MC LBF, supersaturated drug precipitated at the higher drug loads (*i.e.*, 60% and 80% saturations). The rate of drug precipitation from the digesting Type IIIA-MC LBF was faster than that of the Type II MC LBF and sufficient for drug concentrations to reach the solubility limit between 30 – 60 min.

Type IIIB-MC and IV LBFs exhibited lower solubilization capacities on dispersion (0.87 ± 0.02 mg/ml and 0.38 ± 0.01 mg/ml, respectively) when compared to the more lipid-rich Type II-MC and IIIA-MC LBFs. This led to higher drug supersaturation on dispersion, and initiation of precipitation prior to digestion (Fig. 5c and d). Precipitation during the dispersion of Type IIIB-MC LBF was evident at 60% and 80% saturation, but not at 20% and 40%. Digestion further lowered the solubilization capacity to 0.39 ± 0.01 mg/ml, and the attendant increase in supersaturation was consistent with more rapid precipitation during the digestion phase. Due to a lack of digestible lipid content, digestion had only a modest impact on the solubilization capacity of the Type IV LBF (decreasing from 0.38 ± 0.01 mg/ml on dispersion to 0.32 ± 0.01 mg/ml on digestion). Digestion therefore did not stimulate fenofibrate precipitation from the Type IV LBF, nor did it appear to affect the precipitation rate. However, dispersion alone was sufficient to generate significant supersaturation and precipitation at all drug loadings except at the lowest drug load (20%).

Figure 6a presents a 3-dimensional plot that illustrates the dependence of SR^M on drug solubility in the digested formulation (AP_{DIGEST}) and the maximum solubilized drug concentration that can be attained on formulation dispersion (AP_{MAX}). The latter is directly related to the mass of drug in the formulation, which in turn is a function of drug

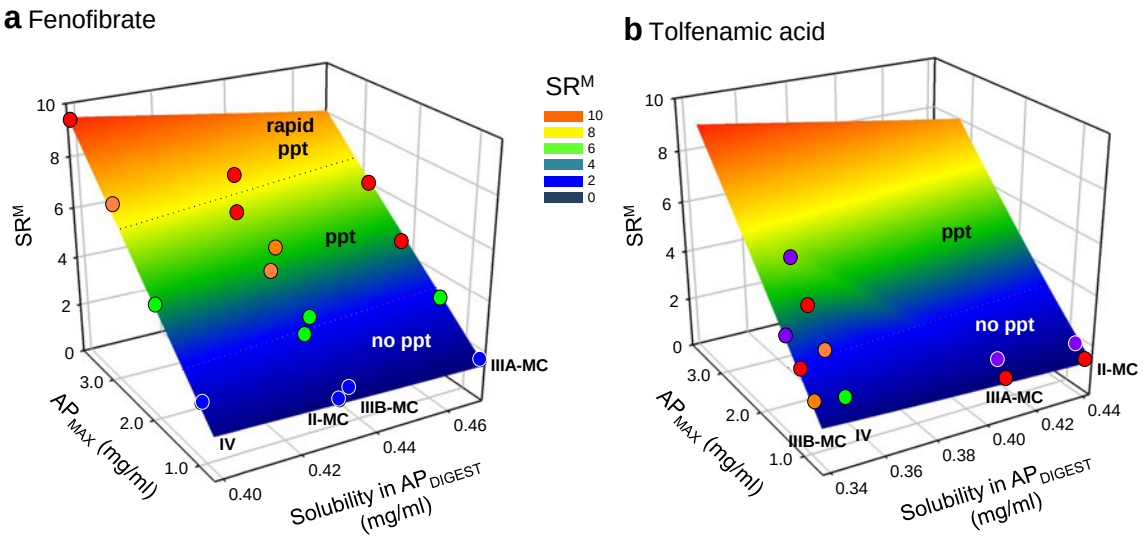

Fig. 6 3-dimensional surface plots to illustrate the relationship between SR^M, AP_{MAX} and drug solubility in the AP_{DIGEST} for (**a**) fenofibrate and (**b**) tolfenamic acid. SR^M is the maximum degree of supersaturation that is attained following 60 min *in vitro* digestion of a lipid-based formulation, and is calculated using Eq. 2 from the ratio between AP_{MAX} (*i.e.*, drug loading divided by test volume) and the solubilization capacity of the AP_{DIGEST} (*i.e.* drug solubility in the digested LBF). With increasing AP_{MAX}, there is a proportional increase in SR^M. The dependency of SR^M on AP_{MAX} increases with decreasing drug solubility in the AP_{DIGEST}. The relationships for the Type II-MC, IIIA-MC, IIIB-MC and IV formulations are shown. Data points (*filled circles*) reflect 4 different drug loadings in each formulation tested in Fig. 5 for fenofibrate and Fig. 7 for tolfenamic acid. Drug loadings were equivalent to 20% (*blue circles*), 40% (*green circles*), 60% (*orange circles*), 80% (*red circles*) and 100% (purple circles for tolfenamic acid only) of the solubility in the formulations. Note that the color scale in the embedded legend refers to the values for SR^M in the response surface and not the data points described above. The *dashed lines* mark the boundaries between different LBF performance categories (no precipitation, precipitation and rapid precipitation). The critical SR^M cut-off for precipitation was similar for both drugs and was ~3.

solubility in the formulation. SR^M provides an indication of the maximum supersaturation 'pressure' that the formulation is under in each test. In a previous publication using danazol as a model poorly water-soluble drug, SR^M was shown to strongly determine drug fate during formulation digestion (20). From Fig. 6a, SR^M (and therefore the risk of precipitation) increases rapidly with increasing drug loading and reduces with increasing drug solubility in the AP_{DIGEST}. In this case, however, drug solubility in digested Type II-MC, IIIA-MC, IIIB-MC and IV LBFs varied by less than 0.1 mg/ml, and as such the major determinant of SR^M was the drug load (as captured in AP_{MAX}).

Overlaid on the 3-dimensional plot are data points (filled circles) that depict the four fenofibrate loadings employed in each of the Type II-MC, IIIA-MC, IIIB-MC and IV LBFs. Thus, for each formulation the drug solubility in the digested formulation (AP_{DIGEST}) is constant, but the four different drug loads provide four data points at increasing AP_{MAX}. From the results in Fig. 5, the dashed lines in Fig. 6a mark the boundaries of LBF performance, with performance grouped according to evidence of; 'no precipitation', 'precipitation' and 'rapid precipitation' (*i.e.*, precipitation that typically commenced during the dispersion phase). Importantly, the no precipitation/precipitation boundary traces along a constant SR^M of ~ 3.

Tolfenamic Acid Containing LBFs

The equivalent data for tolfenamic acid during digestion of Type II-MC, IIIA-MC, IIIB-MC and IV LBFs are shown in Fig. 7. There was no evidence of drug precipitation during the digestion of Type II-MC and IIIA-MC LBFs (Fig. 7a and b). The lack of precipitation was despite drug incorporation at high levels of saturation (up to 100% of drug solubility in the formulation), but can be explained by the fact that drug concentrations in the AP_{DIGEST} were only moderately higher than the solubilization capacity of this phase (the dashed black lines), effectively limiting the degree of supersaturation. For example, at 60 min, the highest SR values were only 1.5 and 1.6 for Type II-MC and IIIA-MC LBFs, respectively. The solubilization capacity of dispersed and digested Type IIIB-MC and IV LBFs were similar to that of the Type II-MC and IIIA-MC LBFs, however because of differences in tolfenamic acid solubility in the original LBFs (Fig. 2), drug loadings were higher at equivalent levels of saturation than previously seen for Type II and IIA MC LBF. The increase in drug load in the Type IIIB-MC and IV LBFs resulted in higher supersaturation on dispersion and digestion and ultimately resulted in drug precipitation from the Type IIIB-MC at a 100% loading and the Type IV LBF above 40% loading.

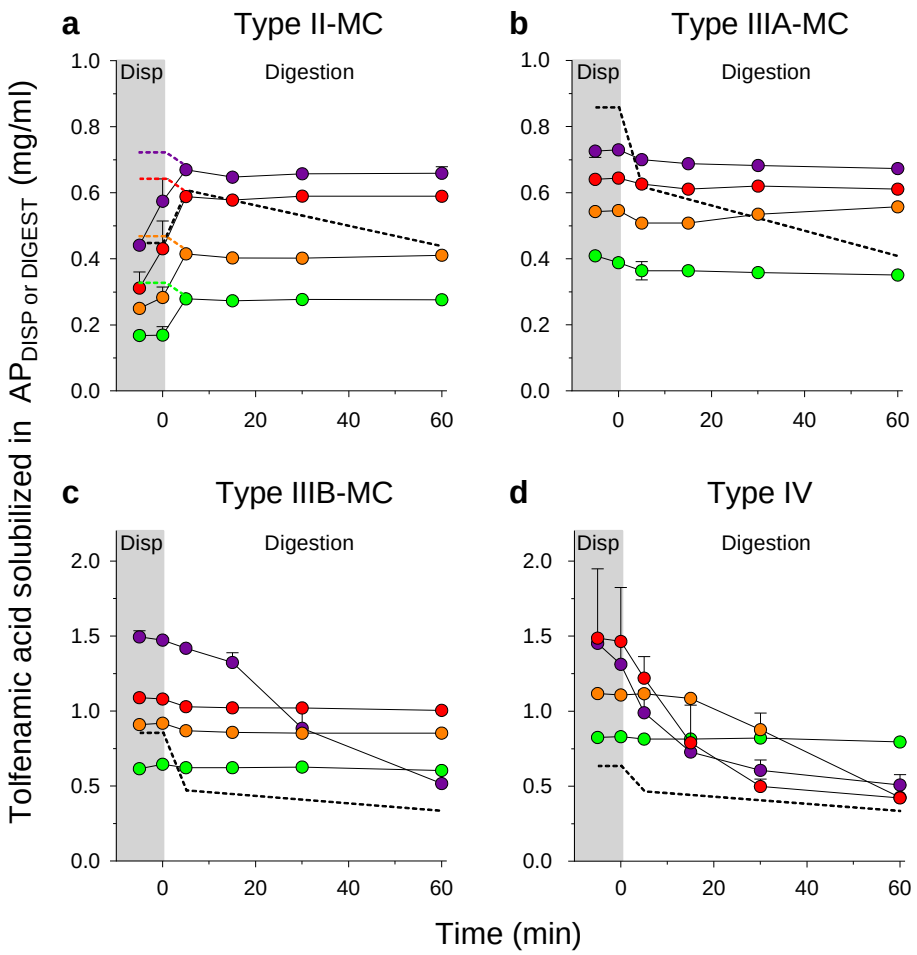

Fig. 7 The effect of tolfenamic acid saturation level in Type II-MC, IIIA-MC, IIIB-MC and IV lipid-based formulations (LBFs) on drug solubilization during 60 min *in vitro* digestion**.** Formulations contained tolfenamic acid at 100% (●), 80% (●), 60% (●) or 40% (●) of solubility in the formulation. Formulation compositions are shown in Fig. 1. All values are expressed as means ($n = 3$) ± 1 SD. The *dashed black* line represents the solubilization capacity of the aqueous phase during LBF dispersion (AP_{DISP}) and digestion (AP_{DIGEST}). The dashed colored lines in panel a represent the total solubilized concentration of tolfenamic acid (drug in AP_{DISP} plus the phase-separated oil phase).

SR^M values for tolfenamic acid are plotted in Fig. 6b in a manner analogous to that described previously for fenofibrate (*i.e.*, Fig. 6a). A comparison of the plots for both drugs highlights that tolfenamic acid LBFs generally gave rise to smaller SR^M values when compared to the equivalent fenofibrate formulations. As the solubilization capacities of the digested LBFs for fenofibrate and tolfenamic acid were similar (i.e. between 0.34-0.48 mg/ml), differences in SR^M stemmed primarily from differences in drug loading. Despite the differences in fenofibrate and tolfenamic acid solubility in the LBFs, however, the fate of the both drugs following digestion of the LBFs was strongly related to SR^M with evidence of precipitation only above a SR^M threshold value of ~3.

Solid-State Analysis of the Fenofibrate and Tolfenamic Acid Precipitate Isolated During *In Vitro* Digestion

To determine the physical form in which fenofibrate and tolfenamic acid precipitated during *in vitro* digestion, isolated pellet phases (containing the drug precipitate) from selected digestion experiments were analyzed by polarized light microscopy (PLM) and x-ray powder diffraction (XRPD). For fenofibrate (Fig. 8), PLM confirmed the presence of fenofibrate crystals in all analyzed drug precipitates. A progressive decrease in the crystal size from IIIA-MC > IIIB-MC > IV was also evident, and occurred coincidently with increasing SR^M. Principal peaks identified in the XRPD diffractograms in the original crystalline material at 11.9^0 (2θ), 14.4^0 (2θ), 16.2^0 (2θ), 16.7^0 (2θ) and 22.2^0 (2θ) [consistent with those reported previously (33)] were also evident in each of the analyzed pellets, confirming fenofibrate precipitation as the thermodynamically stable crystal polymorph.

PLM also confirmed that tolfenamic acid precipitates contained crystalline drug (Fig. 9). Crystals were predominantly rod-shaped and showed some evidence of decreasing size in the order: IIIB-MC (100%) > IV (80%) > IV (100%). This was also consistent with the data obtained for fenofibrate and similarly follows an increase in SR^M. The principal peaks identified in the XRPD diffractograms in the original crystalline material at 11.7^0 (2θ), 15.8^0 (2θ) and 26.9^0 (2θ) [consistent with those reported previously (34)] were also evident in the precipitate from the Type IIIB-MC LBF (Fig. 9a). Diffractograms of the precipitate from the Type IV LBF, at both 80% and 100% saturations (Fig. 9b

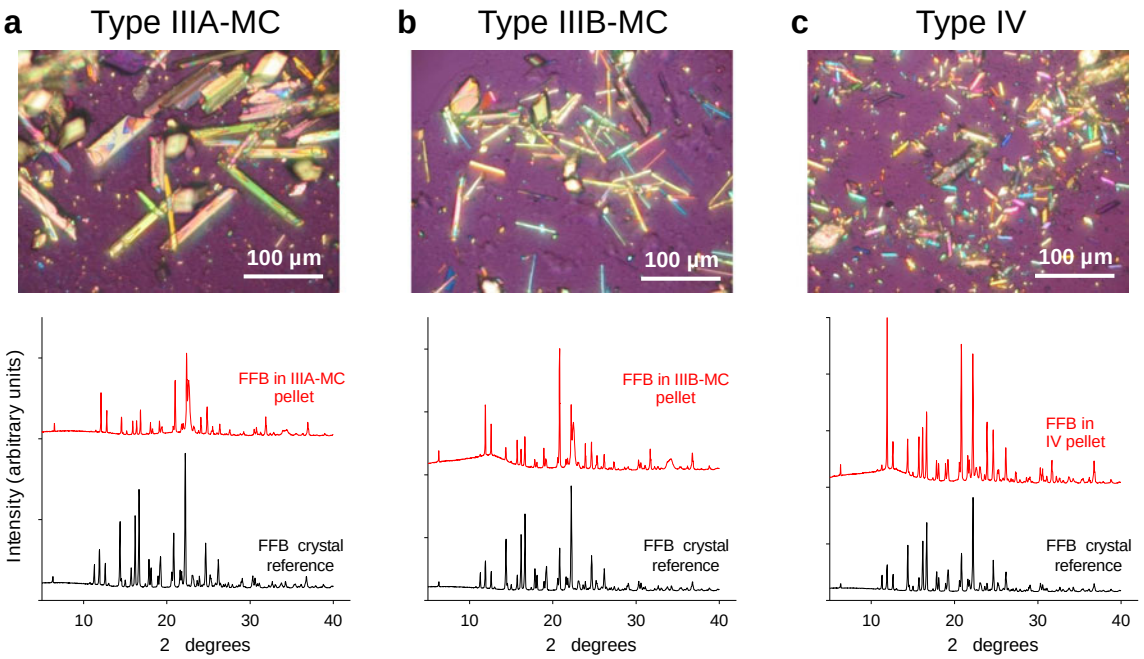

Fig. 8 Analysis of the fenofibrate (FFB) precipitate isolated following *in vitro* digestion of (**a**) Type IIIA-MC, (**b**) Type IIIB-MC and (**c**) Type IV lipid-based formulations (LBFs). All formulations contained fenofibrate at 80% saturation. Polarized light microscopy images were obtained within 1 h of isolating the precipitate. Both polarized light microscopy and x-ray powder diffraction confirmed that fenofibrate precipitated in a crystalline form.

and c), however, did not contain any of the aforementioned peaks. Instead, tolfenamic acid precipitated from the Type IV LBFs as a yellow solid, likely comprising the metastable (form II) polymorph of tolfenamic acid (34,35) that has previously been referred to as tolfenamic acid's "yellow polymorph" (36,37). To verify the form of the yellow precipitate, form II of tolfenamic acid was isolated by the rapid evaporation of a concentrated methanolic solution (see Fig.

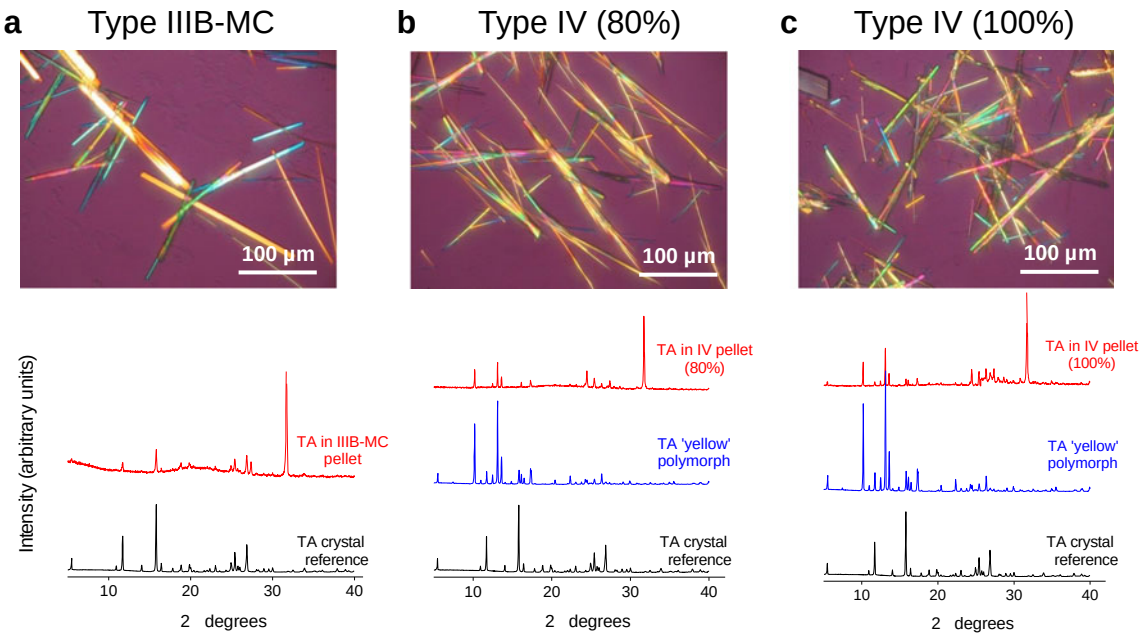

Fig. 9 Analysis of the tolfenamic acid precipitate isolated following *in vitro* digestion of (**a**) Type IIIB-MC and (**b** and c) Type IV lipid-based formulations (LBFs). The Type IIIB-MC LBF contained tolfenamic acid at 100% saturation. The Type IV LBF contained tolfenamic acid at 80% (in **b**) and 100% (in **c**) saturation. Polarized light microscopy images were obtained within 1 h of isolating the precipitate. Both polarized light microscopy and x-ray powder diffraction (XPRD) confirmed that tolfenamic acid precipitated in a crystalline form. The tolfenamic acid precipitate in the case of the Type IIIB-MC LBF was predominantly white in appearance, but was yellow in the case of the Type IV LBFs. XRPD confirmed differences in crystalline diffraction patterns in white and yellow precipitates.

S5 in the Supplementary Material for a photograph of the isolated precipitate) and analyzed by XRPD. Figure 9b and c, show that the diffractogram for form II exhibits unique peaks at 10.2^0 (2θ) and 13.1^0 (2θ). These peaks were present in the diffractograms obtained from the precipitate recovered during digestion of the Type IV formulation at drug loads equivalent to 80% and 100% of drug solubility in the formulation. The data therefore confirm tolfenamic acid precipitation in the metastable form. In each of the tolfenamic acid precipitates isolated from the digestion test (Fig. 9a, b and c), there was evidence of a sharp crystalline peak at 31.7^0 (2θ). This peak is not present in the pure drug diffractograms (both form I and form II), and its origin is unclear.

DISCUSSION

The LFCS Consortium was established in 2009 with the intent of generating standardized conditions for *in vitro* testing of lipid-based formulations (LBFs). In the first publication from the consortium (25), eight LBFs that cover each of the LBF classes described in the Lipid Formulation Classification System (17) were proposed (see Fig. 1) and a set of defined experimental conditions under which *in vitro* digestion testing for LBFs may be conducted was introduced. These conditions provided a basis from which the impact of a number of experimental variables on LBF performance during *in vitro* digestion have subsequently been assessed (20,25,26). In the current submission, the performance of the eight LBFs containing the model drugs, fenofibrate (a highly lipophilic neutral compound) and tolfenamic acid (a poorly water-soluble weak acid) have been evaluated after formulation dispersion and digestion under a range of drug loads in an attempt to better understand the potential for drug supersaturation and precipitation as the formulations are processed in the GI tract. The current studies extend a previous examination of LBFs containing danazol (20) that showed that stimulation of drug precipitation through LBF digestion occurred only when the maximum supersaturation ratio (SR^M) was above a threshold value of ~2.5, irrespective of the composition of the LBF. The present study identifies supersaturation thresholds for both fenofibrate and tolfenamic acid containing LBFs and, despite significant differences in physicochemical properties across the three drugs, suggests that the supersaturation thresholds for danazol, fenofibrate and tolfenamic acid are remarkably consistent (and ~ 2.5 – 3.0). SR^M is therefore emerging as a potential parameter with which to predict drug fate during *in vitro* testing of LBFs, and may assist in discriminating between LBFs based on expected performance during *in vitro* dispersion and digestion.

Fenofibrate *vs.* Tolfenamic Acid Solubility in Type I, II, IIIA/B and IV LBFs is Dictated by Differences in Melting Point

Fenofibrate has high solubility (>95 mg/g) in all the studied LBFs (Fig. 2), with slightly (<1.5-fold) higher solubility in LBFs containing MC lipids and in Type IIIB-MC and IV LBF that contain Transcutol [(in which fenofibrate was highly soluble (243.8 ± 21.4 mg/g at 37°C)]. The solubility of tolfenamic acid was much lower in all formulations and <25 mg/g unless high amounts of hydrophilic surfactants or cosolvent were included. Fenofibrate and tolfenamic acid are both highly lipophilic when assessed by Log P [5.24 (28) and 5.7 (31), respectively], however the melting point of fenofibrate [81°C (27)] is considerably lower than that of tolfenamic acid [212°C (30)] and most likely explains the significantly higher lipid solubility.

Fenofibrate and Tolfenamic Acid Have No Effect on the *In Vitro* Digestibility of Type I, II, IIIA/B and IV LBFs

Consistent with previous studies using danazol (20), the digestion of Type I, II and III LBFs containing MC or LC lipid, and Type IV LBFs was largely insensitive to incorporated tolfenamic acid or fenofibrate (Fig. 3 and Fig. S2 and S3). In the case of fenofibrate, the lack of drug effects on LBF digestion was despite the presence of high absolute drug loadings. This finding is in contrast to a previous study where fenofibrate was suggested to reduce the concentration of titratable fatty acid during the digestion of a fenofibrate-containing LBF based on medium-chain triglyceride (38). An explanation for the discrepancy across these studies is not apparent at this time, however, the lack of an effect of fenofibrate and tolfenamic acid on the digestion of eight different LBFs across a wide range of drug loadings reported here is consistent with previous work (20) and previous unpublished observations in our laboratory that suggest that drug effects on the rate of lipid digestion are uncommon under the present *in vitro* digestion conditions.

The Fate of Incorporated Fenofibrate or Tolfenamic Acid During *In Vitro* LBF Digestion is Dependent on the Maximum Supersaturation ratio (SR^M)

The data in Figs. 5 and 7 describe the impact of drug load on the performance of fenofibrate and tolfenamic acid containing LBF during *in vitro* dispersion and digestion. In the present study, whenever drug precipitation occurred, the precipitate was crystalline (Figs. 8 and 9). This suggests, at least for tolfenamic acid and fenofibrate, that designing LBFs that resist precipitation during dispersion and digestion may be beneficial, since the slow dissolution rate of

crystalline drug is expected to limit absorption. In some instances, tolfenamic acid phase-separated in an alternate metastable crystalline form (*i.e.*, form II). As a higher-energy metastable state, form II exhibits a greater (kinetic) solubility (37). It is therefore possible that the formation of the more water-soluble form may off-set the challenges associated with drug precipitation. The solubility advantage offered by metastable crystal polymorphs (39), however, is less than that of a non-crystalline (amorphous) solid (40) and tolfenamic acid concentrations at the end of experiments where form II was generated (Fig. 7d) were only slightly higher than the solubility of the more stable crystalline form. In contrast to the current data with tolfenamic acid and fenofibrate and previous studies with danazol (14), where drug precipitation from digesting LBFs occurred in a crystalline form, LBFs containing cinnarizine have been suggested to liberate drug in the amorphous form, albeit under different *in vitro* conditions (41). Where drug precipitates in the amorphous form, the problems of redissolution of the solid material are expected to be reduced.

In the current studies using fenofibrate and tolfenamic acid, LC formulations containing even relatively high drug loads were highly resistant to precipitation (Fig. 4). A combination of factors is likely to have contributed to this robust formulation performance. Firstly, digestion of LC lipid containing formulations resulted in the generation of colloidal species with higher solubilization capacities than the equivalent MC formulation. This likely reflects the lower water solubility of the LC digestion products resulting in more effective swelling of the solubilization volume (and therefore drug solubilization capacity) of mixed bile salt-phospholipid-LC lipid digestion product micelles. Secondly, the presence of an undigested/partially dispersed lipid reservoir restricted the maximum concentration of drug that could be attained in the AP_{DIGEST}. Finally, lower drug solubility in the LC formulations limited the total drug quantity that could be dissolved in the formulation and therefore AP_{MAX}. Collectively, these factors reduce the maximum supersaturation ratio (SR^M) and the overall risk of precipitation during LBF dispersion and digestion. In the case of tolfenamic acid, a moderately high intrinsic solubility in the digestion medium at pH 6.5 (73.3 ± 0.6 µg/ml), even in the absence of an LBF, also minimized the degree of supersaturation attained.

In contrast, for formulations containing MC lipids (Type II-MC, IIIA-MC, IIIB-MC) or no lipid (Type IV) increasing the drug load of fenofibrate or tolfenamic acid resulted in increasing precipitation (Figs. 5 and 7). The factors that contributed to higher degrees of supersaturation, and therefore, a greater risk of precipitation were essentially the opposite of that described above for the LC formulations: Firstly, the MC lipid containing formulations and the lipid free Type IV formulation had higher absolute drug loads at each% saturation level (and therefore higher AP_{MAX}) since drug solubility was higher in these formulations when compared to the LC lipid formulations (Fig. 2); secondly, the solubilization capacity of the digested Type II and IIIA/B MC LBFs was lower than that of the LC equivalents as the digestion products from MC lipids are more water soluble and swell bile salt micelles less efficiently (42); finally, rapid digestion of the MC lipids employed (20,25,43) removes the lipid reservoir that can attenuate drug transfer rates into the AP_{DIGEST}. As a consequence, higher drug concentrations and higher degrees of supersaturation were attained in the AP_{DIGEST}, in turn stimulating drug crystallization.

The maximum drug load that could be tolerated without provoking drug crystallization varied according to LBF type and drug, however, the 3-dimensional plots in Fig. 6 reveal trends in performance that appear to be independent of LBF type. In particular, a threshold SR^M value of ~3 appears to mark the point at which supersaturation passes from that which can be maintained ($SR^M < 3$) to that which leads to precipitation ($SR^M > 3$) (the dashed white lines in Fig. 6). Remarkably, the SR^M threshold of ~3 was consistent for Type II-MC, IIIA-MC, IIIB-MC and IV LBFs and applied equally to fenofibrate and tolfenamic acid containing LBFs. The apparent relationship between SR^M and LBF performance during digestion is better depicted in Fig. 10, which plots the% drug solubilized in the AP_{DIGEST} after 60 min digestion as a function of SR^M generated by

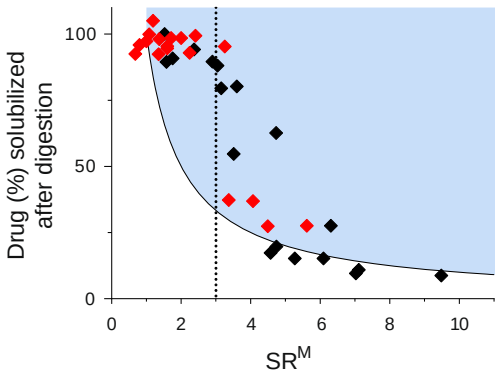

Fig. 10 The relationship identified between the% of drug solubilized in the aqueous colloidal phase (AP_{DIGEST}) after *in vitro* digestion with respect to SR^M. *Black filled symbols* (◆) the performance of LBFs containing fenofibrate. *Red filled symbols* (◆) the performance of LBFs containing tolfenamic acid. The performance of Type IIIA-LC, II-MC, IIIA-MC, IIIB-MC and Type IV LBFs are shown. Individual data points for each formulation type correspond to performance at different drug saturation levels in the formulations assessed over 60 min digestion (except Type IIIA-LC, which are after 30 min digestion). SR^M is calculated from Eq. 2. The *solid line* is the equilibrium curve, *i.e.*, $SR = 1$. *Points* above the curve indicate evidence of supersaturation during *in vitro* digestion. The *vertical dashed* line denotes a SR^M of 3.0, above which there is a trend towards decreasing drug solubilization due to precipitation. A comparison of the above SR^M to those generated using S^M [which captures supersaturation as a function of the change in drug solubility as a LBF is digested (14)] can be found in the Supplementary Material.

Type II-MC, IIIA/B and IV LBFs). The plot highlights a tendency toward decreasing% drug solubilized (due to drug crystallization) above a threshold of SR^M 3 (shown by the dashed vertical line).

The lack of formulation dependency on the fate of the drug in Fig. 10 illustrates that the behavior of the drug in the digestion tests was primarily governed by the supersaturation ratio. This is in-line with classical nucleation theory that suggests a relationship between the degree of supersaturation and the propensity for crystal nuclei formation (21,22). The driving force towards precipitation/crystallization with increasing supersaturation ratio is apparent in Fig. 10 by comparison of the vertical distance between the maximum drug concentration (*i.e.*, the 100% solubilized value) and the solid curved line that represents the drop in concentration expected if drug precipitation is sufficient to remove all supersaturation (*i.e.*, SR = 1). Formulations that are displaced vertically above the solid line are supersaturated and the distance from the SR = 1 line provides an indication of the relative magnitude of supersaturation.

Type I-LC, II-LC and I-MC LBFs have been omitted from the comparison in Fig. 10 since these LBFs were only partially digested *in vitro* and the undigested lipid phase limited the proportion of the dose entering the AP_{DIGEST}. SR^M values for these LBF may however be estimated, by correcting for the proportion of the drug dose that exists in the lipid phase by multiplying AP_{MAX} by the% of drug dose present in the AP_{DIGEST}. Corrected SR^M values for all LC LBFs containing either fenofibrate or tolfenamic acid were <3.05, consistent with the lack of drug precipitation during the digestion of these LBFs (Fig. 4). This suggests that a threshold SR^M of 3 in determining the propensity for precipitation may apply to both LC and MC formulations. Interestingly, as drug saturation levels in the LC formulations examined here were 80% and 100%, it seems likely that for LC LBFs it is difficult to generate SR^M values above the threshold value if drug is present in the formulation at concentrations below equilibrium solubility. This may help to explain previous descriptions of enhanced *in vivo* performance of LC LBF when compared to MC LBF across a range of drug loads (5,24,44). Another descriptor of supersaturation during LBF digestion is the parameter S^M which is analogous to SR^M but also accounts for the changes in drug solubility during the course of the digestion test (14). However, as solubilities measured in this study after 5 min and 60 min digestion were not to different (in many cases reflecting rapid LBF digestion), calculated SR^M and S^M values, and the overall trend in the results using either descriptor were comparable (see Fig S6 and S7 in the Supplementary Material).

The identification of a SR^M threshold that defines the highest supersaturation ratio that can be maintained without precipitation is consistent with our previous work using equivalent LBFs containing danazol (20). For danazol, drug precipitation was evident above a SR^M threshold of ~2.5. This is remarkably similar to the threshold SR^M of 3 identified here for both fenofibrate and tolfenamic acid, and is in spite of significant differences in a number of molecular descriptors that are commonly used as indicators of crystallization tendency. These include molecular weight, number of rotatable bonds, polar surface area, molecular symmetry and melting point (45,46). In addition, the results of the present study in conjunction with previous findings from the LFCS Consortium (20) and other studies in our laboratory (47) suggest that SR^M is also largely independent of LBF composition and experimental test conditions, further highlighting the utility of this parameter in describing LBF performance on digestion. Notwithstanding these general observations of *in vitro* performance, it is apparent that additional properties are likely to play an important role in the *in vivo* performance of LBF including the rate of absorption relative to the rate of precipitation (48). Indeed, where absorption is rapid, only relatively brief periods of supersaturation may be sufficient to drive increases in drug flux. Recent studies have elegantly exemplified the realization that drug absorption inevitably decreases the degree of supersaturation, and that a supersaturation ratio measured *in vitro*, in the absence of an absorption sink, is likely to overestimate *in vivo* supersaturation and precipitation potential (49,50).

Drug Precipitation Kinetics During Digestion is Dependent on SR^M

The kinetics of drug precipitation during formulation processing (as opposed to the extent of precipitation described above) are also an important determinant of formulation performance, and were examined in more detail by repeat sampling of the digests as a function of time (Figs. 5 and 7). The supersaturation kinetics of fenofibrate-containing LBFs are also captured in Fig. 11, which plots the% fenofibrate dose that remained solubilized after (a) 10 min dispersion, and after (b) 5 min (c), 15 min (d) 30 min and (e) 60 min of digestion of II-MC, IIIA-MC, IIIB-MC and IV formulations, as a function of SR^M (fenofibrate data points in Fig. 10 are reproduced in Fig. 11e). SR^M values were calculated using Eq. 2 and employed the solubility values measured at each of respective time points during dispersion or digestion. In addition to the dose, the solubilization capacity of the digested LBF (*i.e.*, the AP_{DIGEST}) strongly affects SR^M, and therefore, the position of the data points in these plots. For example, many of the SR^M values in the dispersion phase (Fig. 11a) are low and <3, but due to digestion subsequently lowering the solubilization capacity of the digested LBF (Fig. 11b–e), the majority of these points shift along the x-axis to higher SR^M values with time, increasing precipitation risk. The plots also highlight the fact that the rate of fenofibrate crystallization is generally low at low SR^M values. This observation is most evident on scrutiny of the initial 10 min dispersion phase (Fig. 11a) where the majority

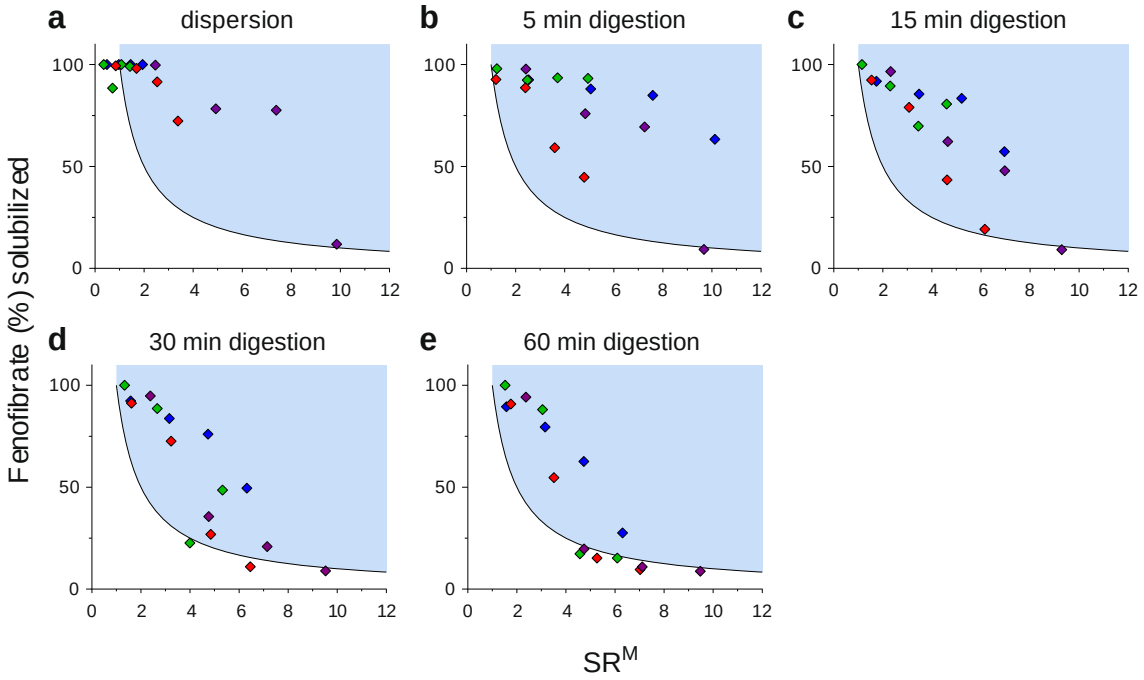

Fig. 11 The kinetics of fenofibrate crystallization from the supersaturated state generated by *in vitro* digestion of Type II-MC, IIIA-MC, IIIB-MC and IV lipid-based formulations (LBFs) plotted with respect to SR^M. Symbols represent Type II-MC (*blue symbols*), Type IIIA-MC (*green symbols*), Type IIIB-MC (*red symbols*), and Type IV (*purple symbols*) LBFs. (**a**–**e**) % of fenofibrate that remained in solution at various time points during the tests. SR^M is calculated from Eq. 2. The *solid line* is the equilibrium curve, *i.e.*, SR = 1. *Points* above the curve indicate evidence of supersaturation.

of SR^M values are <3 and most of the drug remains supersaturated. During the digestion phase, SR^M values increase to ~3 to 5, resulting in precipitation initiation, however the rate of precipitation is sufficiently low that some degree of supersaturation is still evident by the end of the test (60 min). SR^M therefore provides an indication of both the overall risk of drug precipitation and some information on the kinetic stability of the supersaturated state, with decreasing SR^M leading to increased kinetic stability of drug in the digestion lipid phases. The potential for SR^M to inform the kinetic stability of supersaturation in digested LBFs is consistent with models in the literature that relate the rate of crystal growth to supersaturation ratio (51).

Though the thermodynamic basis of the SR^M threshold is not fully understood, classical nucleation theory (CNT) suggests that the thermodynamic barrier to nucleation (*i.e.*, the activation energy) decreases with increasing supersaturation ratio until a critical point is reached where the activation barrier is negligible and nucleation is spontaneous (52,53). The CNT therefore provides a basis for a threshold supersaturation, such as the SR^M threshold described here and in previous work (20). It is possible that this threshold may represent the ratio between the solubility of metastable (amorphous) drug and crystalline drug within the colloids formed during digestion (54) since previous work has shown that crystal growth mechanisms are more rapid and much less ordered as concentrations equivalent to the amorphous drug solubility are reached (55,56).

Supersaturation Parameters such as SR^M May Aid LBF Design by Informing Maximal Drug Loadings

Finally, SR^M provides an opportunity to predict maximal drug loads in LBF without the need to run *in vitro* digestion tests for each formulation. Thus, digestion of a blank formulation and measurement of drug solubility in the AP_{DIGEST} provides a baseline from which SR^M can be calculated for any potential drug load. SR^M at different drug loads can subsequently be simulated by calculation of AP_{MAX} (from a knowledge of drug load and digest volume, where drug load is maximally limited by drug solubility in the formulation) and comparison with drug solubility in AP_{DIGEST}. The current data suggest that drug loads up to those that result in a SR^M of 3 are likely to be better tolerated.

CONCLUSIONS

Increasing LBF drug load can significantly impact on formulation performance during digestion through effects on supersaturation and precipitation risk. The present study provides evidence that the fate of structurally diverse drugs in a wide range of LBFs during digestion is captured consistently by the maximum supersaturation ratio (SR^M). SR^M defines the maximum extent of supersaturation in a digested LBF *in vitro*. Below a threshold SR^M of 3, LBFs prove

effective in providing high concentrations of supersaturated drug, however, above this SR^M threshold, supersaturation cannot be sustained, and drug precipitates.

This capacity for small differences in supersaturation ratio to significantly alter drug solubilization by lipid formulations highlights the delicate balance between 'beneficial' degrees of supersaturation, that are expected to enhance drug absorption *in vivo*, and 'detrimental' supersaturation, that promotes drug precipitation, and may reduce drug absorption. *In vitro* digestion tests that afford insights into the fate of supersaturated drug during LBF digestion therefore provide useful tools in LBF design and selection - the conditions of such *in vitro* tests are currently being standardized by the LFCS Consortium.

ACKNOWLEDGMENTS AND DISCLOSURES

This study results from a joint collaboration between members of the LFCS Consortium funded primarily by Capsugel and Sanofi R & D, with additional funding from Gattefossé, Merck Serono, NicOx, Roche, Bristol-Myers Squibb and Actelion. The authors would like to thank Dr. Laura Gordon and the Chemical Engineering department at Melbourne University for the XRPD analysis, and Rhiannon Smythe and Samuel Wood for determining the fenofibrate solubilities in the digested lipid formulations.

REFERENCES

1. Porter CJH, Trevaskis NL, Charman WN. Lipids and lipid-based formulations: optimizing the oral delivery of lipophilic drugs. Nat Rev Drug Discov. 2007;6:231–48.
2. Williams HD, Trevaskis NL, Charman SA, Shanker RM, Charman WN, Pouton CW, *et al.* Strategies to address low drug solubility in discovery and development. Pharmacol Rev. 2013;65:315–499.
3. Hauss DJ. Enhancing the bioavailability of poorly water-soluble drugs. New York: Informa Healthcare; 2007.
4. Charman SA, Charman WN, Rogge MC, Wilson TD, Dutko FJ, Pouton CW. Self-emulsifying drug delivery systems: formulation and biopharmaceutic evaluation of an investigational lipophilic compound. Pharm Res. 1992;9:87–93.
5. Porter CJH, Kaukonen AM, Boyd BJ, Edwards GA, Charman WN. Susceptibility to lipase-mediated digestion reduces the oral bioavailability of danazol after administration as a medium-chain lipid-based microemulsion formulation. Pharm Res. 2004;21:1405–12.
6. Porter CJH, Pouton CW, Cuine JF, Charman WN. Enhancing intestinal drug solubilisation using lipid-based delivery systems. Adv Drug Deliv Rev. 2008;60:673–91.
7. Constantinides PP, Wasan KM. Lipid formulation strategies for enhancing intestinal transport and absorption of P-glycoprotein (P-gp) substrate drugs: *in vitro*/*in vivo* case studies. J Pharm Sci. 2007;96:235–48.
8. Lindmark T, Kimura Y, Artursson P. Absorption enhancement through intracellular regulation of tight junction permeability by medium chain fatty acids in Caco-2 cells. J Pharmacol Exp Ther. 1998;284:362–9.
9. Goole J, Lindley DJ, Roth W, Carl SM, Amighi K, Kauffmann JM, *et al.* The effects of excipients on transporter mediated absorption. Int J Pharm. 2010;393:17–31.
10. Trevaskis NL, Porter CJH, Charman WN. An examination of the interplay between enterocyte-based metabolism and lymphatic drug transport in the rat. Drug Metab Dispos. 2006;34:729–33.
11. Patel JP, Brocks DR. The effect of oral lipids and circulating lipoproteins on the metabolism of drugs. Expert Opin Drug Metab Toxicol. 2009;5:1385–98.
12. Trevaskis NL, Charman WN, Porter CJH. Lipid-based delivery systems and intestinal lymphatic drug transport: a mechanistic update. Adv Drug Deliv Rev. 2008;60:702–16.
13. O'Driscoll CM. Lipid-based formulations for intestinal lymphatic delivery. [Review] [85 refs]. Eur J Pharm Sci. 2002;15:405–15.
14. Anby MU, Williams HD, McIntosh M, Benameur H, Edwards GA, Pouton CW, *et al.* Lipid digestion as a trigger for supersaturation: *in vitro* and *in vivo* evaluation of the utility of polymeric precipitation inhibitors in self emulsifying drug delivery systems. Mol Pharm. 2012;9:2063–79.
15. Gao P, Akrami A, Alvarez F, Hu J, Li L, Ma C, *et al.* Characterization and optimization of AMG 517 Supersaturatable Self-Emulsifying Drug Delivery System (S-SEDDS) for improved oral absorption. J Pharm Sci. 2009;98:516–28.
16. Brouwers J, Brewster ME, Augustijns P. Supersaturating drug delivery systems: the answer to solubility-limited oral bioavailability? J Pharm Sci. 2009;98:2549–72.
17. Pouton CW. Formulation of poorly water-soluble drugs for oral administration: physicochemical and physiological issues and the lipid formulation classification system. Eur J Pharm Sci. 2006;29:278–87.
18. Yeap YY, Trevaskis NL, Quach T, Tso P, Charman WN, and Porter CJH. Intestinal bile secretion promotes drug absorption from lipid colloidal phases *via* induction of supersaturation. Mol Pharmaceut. 2013. doi:10.1021/mp3006566
19. Yeap YY, Trevaskis NL, and Porter CJH. The acidic microclimate of the intestinal unstirred water layer can promote drug absorption from long-chain mixed micelles *via* induction of supersaturation at the absorptive site. Pharm Res. This issue:2013.
20. Williams HD, Anby MU, Sassene P, Kleberg K, Bakala N'Goma JC, Calderone M, *et al.* Toward the establishment of standardized *in vitro* tests for lipid-based formulations: 2) The effect of bile salt concentration and drug loading on the performance of Type I, II, IIIA, IIIB and IV formulations during *in vitro* digestion. Mol Pharm. 2012;9:3286–300.
21. James PF. Kinetics of crystal nucleation in silicate-glasses. J Non-Cryst Solids. 1985;73:517–40.
22. Turnbull D, Fischer JC. Rate of nucleation in condensed systems. J Chem Phys. 1949;17:71–3.
23. Cuine JF, Charman WN, Pouton CW, Edwards GA, Porter CJH. Increasing the proportional content of surfactant (Cremophor EL) relative to lipid in self-emulsifying lipid-based formulations of danazol reduces oral bioavailability in beagle dogs. Pharm Res. 2007;24:748–57.
24. Dahan A, Hoffman A. Use of a dynamic *in vitro* lipolysis model to rationalize oral formulation development for poor water soluble drugs: correlation with *in vivo* data and the relationship to intra-enterocyte processes in rats. Pharm Res. 2006;23:2165–74.
25. Williams HD, Sassene P, Kleberg K, Bakala N'Goma JC, Calderone M, Jannin V, *et al.* Toward the establishment of standardized *in vitro* tests for lipid-based formulations: 1) Method parameterization and comparison of *in vitro* digestion profiles across a range of representative formulations. J Pharm Sci. 2012;101:3360–80.
26. Sassene P, Kleberg K, Williams HD, Bakala N'Goma JC, Calderone M, Jannin V, *et al.* Toward the establishment of standardized *in vitro* tests for lipid-based formulations: 3) Effect of calcium and pancreatin concentration. In preparation 2013.

27. Van Speybroeck M, Mellaerts R, Mols R, Do Thi T, Martens JA, Van Humbeeck J, *et al.* Enhanced absorption of the poorly soluble drug fenofibrate by tuning its release rate from ordered mesoporous silica. Eur J Pharm Sci. 2010;41:623–30.
28. Munoz A, Guichard JP, Reginault P. Micronized fenofibrate. Atherosclerosis. 1994;110:S45–8.
29. Vogt M, Kunath K, Dressman JB. Dissolution enhancement of fenofibrate by micronization, cogrinding and spray-drying: Comparison with commercial preparations. Eur J Pharm Biopharm. 2008;68:283–8.
30. Bergstroem CAS, Wassvik CM, Johansson K, Hubatsch I. Poorly soluble marketed drugs display solvation limited solubility. J Med Chem. 2007;50:5858–62.
31. Osterberg T, Svensson M, Lundahl P. Chromatographic retention of drug molecules on immobilised liposomes prepared from egg phospholipids and from chemically pure phospholipids. Eur J Pharm Sci. 2001;12:427–39.
32. Fagerberg JH, Al-Tikriti Y, Ragnarsson G, Bergstrom CAS. Ethanol effects on apparent solubility of poorly soluble drugs in simulated intestinal fluid. Mol Pharm. 2012;9:1942–52.
33. Heinz A, Gordon KC, McGoverin CM, Rades T, Strachan CJ. Understanding the solid-state forms of fenofibrate - A spectroscopic and computational study. Eur J Pharm Biopharm. 2009;71:100–8.
34. Mattei A, Li T. Polymorph formation and nucleation mechanism of tolfenamic acid in solution: an investigation of pre-nucleation solute association. Pharm Res. 2012;29:460–70.
35. Anderson KV, Larsen S, Alhede B, Gelting N, Buchardt O. Characterization of two polymorphic forms of tolfenamic acid, N-(2-Methyl-3-chlorophenyl)anthranilic acid: their crystal structures and relative stabilities. J Chem Soc Perkin Trans. 1989;2:1443–7.
36. Thybo P, Kristensen J, Hovgaard L. Characterization and physical stability of tolfenamic Acid-PVP K30 solid dispersions. Pharm Dev Technol. 2007;12:43–53.
37. Surov AO, Szterner P, Zielenkiewicz W, Perlovich GL. Thermodynamic and structural study of tolfenamic acid polymorphs. J Pharm Biomed Anal. 2009;50:831–40.
38. Arnold YE, Imanidis G, Kuentz M. Study of drug concentration effects on *in vitro* lipolysis kinetics in medium-chain triglycerides by considering oil viscosity and surface tension. Eur J Pharm Sci. 2011;44:351–8.
39. Pudipeddi M, Serajuddin ATM. Trends in solubility of polymorphs. J Pharm Sci. 2005;94:929–39.
40. Murdande SB, Pikal MJ, Shanker RM, Bogner RH. Solubility advantage of amorphous pharmaceuticals, Part 3: is maximum solubility advantage experimentally attainable and sustainable? J Pharm Sci. 2011;100:4349–56.
41. Sassene PJ, Knopp MM, Hesselkilde JZ, Koradia V, Larsen A, Rades T, *et al.* Precipitation of a poorly soluble model drug during *in vitro* lipolysis: characterization and dissolution of the precipitate. J Pharm Sci. 2010;99:4982–91.
42. Kossena GA, Boyd BJ, Porter CJH, Charman WN. Separation and characterization of the colloidal phases produced on digestion of common formulation lipids and assessment of their impact on the apparent solubility of selected poorly water-soluble drugs. J Pharm Sci. 2003;92:634–48.
43. Sek L, Porter CJH, Kaukonen AM, Charman WN. Evaluation of the *in-vitro* digestion profiles of long and medium chain glycerides and the phase behaviour of their lipolytic products. J Pharm Pharmacol. 2002;54:29–41.
44. Porter CJH, Kaukonen AM, Taillardat-Bertschinger A, Boyd BJ, O'Connor JM, Edwards GA, *et al.* Use of *in vitro* lipid digestion data to explain the *in vivo* performance of triglyceride-based oral lipid formulations of poorly water-soluble drugs: studies with halofantrine. J Pharm Sci. 2004;93:1110–21.
45. Baird JA, Van Eerdenbrugh B, Taylor LS. A classification system to assess the crystallization tendency of organic molecules from undercooled melts. J Pharm Sci. 2010;99:3787–806.
46. Mahlin D, Ponnambalam S, Hockerfelt MH, Bergstrom CAS. Toward in silico prediction of glass-forming ability from molecular structure alone: a screening tool in early drug development. Mol Pharm. 2011;8:498–506.
47. Devraj R, Williams HD, Warren DB, Porter CJH, and Pouton CW. Effect of different nonionic surfactants in self-emulsifying lipid formulations on supersaturation during *in vitro* digestion. Submitted, 2013.
48. Williams HD, Pouton CW, and Porter CJH. Lipid-based formulations and drug supersaturation: Harnessing the unique benefits of the lipid digestion/absorption pathway. Pharm Res. This issue:2013.
49. Bevernage J, Brouwers J, Annaert P, Augustijns P. Drug precipitation-permeation interplay: supersaturation in an absorptive environment. Eur J Pharm Biopharm. 2012;82:424–8.
50. Bevernage J, Brouwers J, Brewster ME, and Augustijns P. Evaluation of gastrointestinal drug supersaturation and precipitation: Strategies and issues. Int J Pharm. 2012. doi:10.1016/j.ijpharm.2012.11.026
51. Judge RA, Johns MR, White ET. Protein-purification by bulk crystallization - The recovery of ovalbumin. Biotechnol Bioeng. 1995;48:316–23.
52. Vekilov PG. Nucleation. Cryst Growth Des. 2010;10:5007–19.
53. Kashchiev D, von Rosmalen GM. Review: nucleation in solutions revisited. Cryst Res Technol. 2003;38:555–74.
54. Williams HD, Hergaden B, and Porter CJH. Drug supersaturation in digested lipid-based drug delivery systems. AAPS J. S2:2012.
55. Alonzo DE, Raina S, Zhou D, Gao Y, Zhang GGZ, Taylor LS. Characterizing the impact of hydroxypropylmethyl cellulose on the growth and nucleation kinetics of felodipine from supersaturated solutions. Cryst Growth Des. 2012;12:1538–47.
56. Ilevbare GA, Liu H, Edgar KJ, Taylor LS. Inhibition of solution crystal growth of ritonavir by cellulose polymers - factors influencing polymer effectiveness. Cryst Eng Comm. 2012;14:6503–14.